nature chemistry

ARTICLES

PUBLISHED ONLINE: 20 FEBRUARY 2011 | DOI: 10.1038/NCHEM.988

The role of long-lived reactive oxygen intermediates in the reaction of ozone with aerosol particles

Manabu Shiraiwa[1], Yulia Sosedova[2,3], Aurélie Rouvière[2], Hong Yang[1], Yingyi Zhang[1], Jonathan P. D. Abbatt[4], Markus Ammann[2] and Ulrich Pöschl[1]*

The heterogeneous reactions of O_3 with aerosol particles are of central importance to air quality. They are studied extensively, but the molecular mechanisms and kinetics remain unresolved. Based on new experimental data and calculations, we show that long-lived reactive oxygen intermediates (ROIs) are formed. The chemical lifetime of these intermediates exceeds 100 seconds, which is much longer than the surface residence time of molecular O_3 ($\sim 10^{-9}$ s). The ROIs explain and resolve apparent discrepancies between earlier quantum mechanical calculations and kinetic experiments. They play a key role in the chemical transformation and adverse health effects of toxic and allergenic air-particulate matter, such as soot, polycyclic aromatic hydrocarbons and proteins. ROIs may also be involved in the decomposition of O_3 on mineral dust and in the formation and growth of secondary organic aerosols. Moreover, ROIs may contribute to the coupling of atmospheric and biospheric multiphase processes.

Reactive oxygen species (ROS) play important roles in both atmospheric chemistry and physiological processes: O_3 photochemistry, oxidative self-cleaning of the atmosphere, biological ageing, metabolism and oxidative stress[1–4]. In physiology and biochemistry, the umbrella term ROS is defined broadly to comprise a wide range of oxygen-centred and related free radicals, ions and molecules[1–3]. As illustrated in Fig. 1, different types of ROS are closely coupled by radical reactions and cyclic transformation[5–7]. The coupling and exchange of atmospheric and physiological ROS can proceed through various interfaces, such as plant surfaces and the human respiratory tract (emission and deposition of trace gases and particle deposition). Also, the biomedical definition of ROS includes reactive nitrogen species (RNS), such as NO, NO_2 and ONO_2^- (ref. 3). In atmospheric science, however, RNS are usually treated separately from oxy, hydroxy and peroxy radicals[7,8]. For clarity, we adopt the term ROIs to describe the subset of ROS potentially involved in the reaction of O_3 with aerosol particles, including organic and inorganic species, with reactive oxygen atoms or groups (O, RO, RO_2 and so on).

Heterogeneous reactions of O_3 with aerosol particles are studied extensively, but the molecular mechanism and kinetics remain unresolved[9–15]. Among the organic aerosol components that react readily with O_3, polycyclic aromatic hydrocarbons (PAHs) are one of the most prominent groups in terms of health effects. They are an integral component of soot and related carbonaceous combustion aerosol particles (in the submicron range) that can penetrate deep into human lungs[7]. Chemical transformation can change the toxicity of PAHs and modify the hygroscopic properties and climate effects of combustion aerosol particles[6,7]. PAH oxidation products (quinones, phenols and so on) are also involved in physiological processes that lead to the adverse health effects of traffic-related air pollution[3,5,16,17]. Several studies show that O_3 can also promote the nitration of protein molecules contained in primary biological aerosol particles, such as pollen and fungal spores[18–20]. This post-translational modification can enhance the allergenic potential of proteins. It provides a molecular rationale for the enhancement of allergic diseases by traffic-related air pollution in urban and rural environments observed in epidemiological studies, but the molecular mechanism remains to be elucidated[18,21,22].

Laboratory studies of the heterogeneous reaction of O_3 with PAHs adsorbed on soot and other substrates generally show a non-linear dependence of the first-order PAH decay rate coefficient on gas-phase O_3 concentration, which is consistent with a Langmuir–Hinshelwood (LH) reaction mechanism[12,23], in which an adsorbed O_3 molecule reacts with the PAH in a surface reaction. The O_3

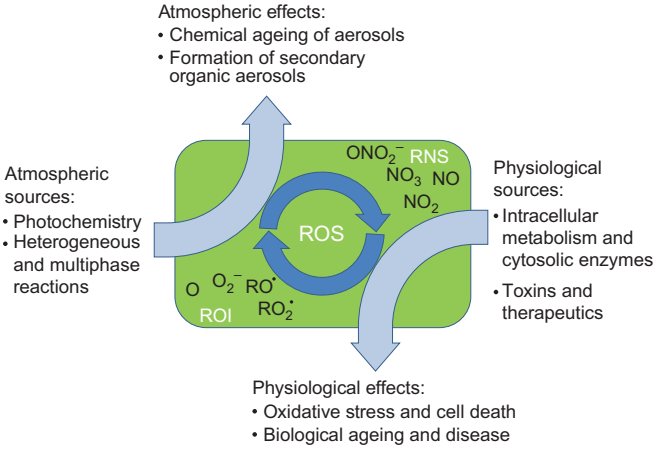

Figure 1 | Illustration of the atmospheric and physiological sources, coupling and effects of ROS. These are defined broadly to include ROIs as well as RNS.

[1]Max Planck Institute for Chemistry, Department of Biogeochemistry, PO Box 3060, 55128, Mainz, Germany, [2]Paul Scherrer Institut, Laboratory of Radiochemistry and Environmental Chemistry, Villigen, CH-5232, Switzerland, [3]Department of Chemistry and Biochemistry, University of Bern, Freiestrasse 3, Bern CH-3012, Switzerland, [4]University of Toronto, Department of Chemistry, 80 St George Street, Toronto, Ontario M5S 3H6, Canada.
*e-mail: u.poschl@mpic.de

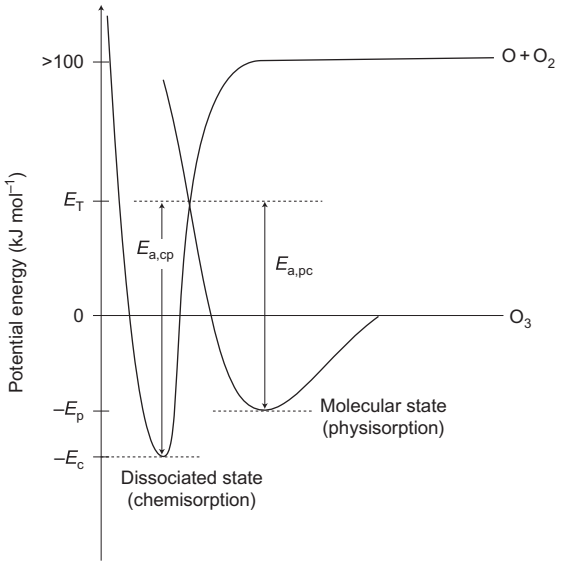

Figure 2 | Lennard-Jones potential energy diagram for the adsorption of molecular and dissociated O_3. The physisorbed O_3 molecule (binding energy E_p) can be desorbed thermally to the gas phase with a desorption lifetime of nanoseconds, or it can overcome an activation barrier ($E_{a,pc}$), go through a transition state (potential energy E_T) and enter into a dissociated state (binding energy E_c). The process can be reversed by overcoming the activation barrier from chemisorption to physisorption ($E_{a,cp}$). The horizontal axis represents the distance from the surface.

surface-residence time or desorption lifetime (τ_{d,O_3}) inferred from kinetic data, assuming a simple LH reaction between adsorbed O_3 and surface molecules, are in the range 10^{-2} s to 10 s (refs 24,25). However, according to quantum mechanical calculations based on density functional theory (DFT), the desorption lifetime of O_3 on PAH[11] or graphene[26] should be only nanoseconds, which is more than six orders of magnitude less. This indicates that the DFT simulations address a different step and state of O_3 adsorption than the reaction kinetic experiments. In this study we resolve the apparent discrepancy using a new kinetic modelling approach that takes into account intermediate processes of O_3 decomposition on the surface.

Results and discussion

ROIs in the oxidation of PAHs. Figure 2 shows a Lennard-Jones potential energy diagram[27] for the adsorption of O_3. It comprises one curve that describes the weak interaction of molecular O_3 with the surface (physisorption) and another that describes the stronger interaction and dissociation of O_3 at the surface (chemisorption). Figure 2 illustrates the thermodynamic conditions for the initial steps of the heterogeneous reaction of gaseous O_3. The weakly bound physisorbed O_3 molecule (binding energy E_p) can be desorbed thermally to the gas phase with a desorption lifetime of nanoseconds, or it can overcome an activation barrier ($E_{a,pc}$), undergo dissociation and enter into a state of stronger binding to the surface (E_c, Fig. 2). The transition state from molecular to dissociated O_3 may be a primary ozonide or a trioxyl diradical[11,28]. The dissociation products are molecular oxygen[29,30] and a ROI, such as a chemisorbed oxygen atom bound to the delocalized π-electrons of an aromatic surface[11,28]. In a further reaction step, the ROIs can form stable products, for example oxygenated PAHs with hydroxyl, carbonyl and other functional groups[7]. Alternatively, the ROIs may be lost by self-reaction or reactions with other chemical species. In surface and materials science, chemisorbed oxygen atoms on aromatic surfaces are often designated as 'epoxide-like' groups[11,26,28,31,32]. However, the oxygen atoms in these 'epoxide-like' groups reside above the aromatic system, which implies that the electronic structure and chemical properties are different from those of classical epoxides[33].

Figure 3 shows experimental data[12] and model results for the heterogeneous ozonolysis of benzo[*a*]pyrene (BaP, $C_{20}H_{12}$), one of the most toxic PAH priority pollutants[7]. The experiments were performed with soot aerosol particles coated in BaP[12] and the model calculations were performed with a kinetic double-layer surface model (K2-SURF)[24] using parameters as detailed in Supplementary Table 1. Figure 3a shows the first-order BaP decay rate coefficient ($k_{s,PAH}$) and Fig. 3b shows the adsorbate surface coverage (θ_s) plotted against the gas-phase O_3 concentration ($[O_3]_g$). The experimentally observed nonlinear dependence of $k_{s,PAH}$ and θ_s on $[O_3]_g$ can be reproduced under the assumption of a simple LH reaction between BaP and reversibly adsorbed O_3 with a very long desorption lifetime ($\tau_{d,O_3} = 16$ s) (ref. 12). If, however, we use a more reasonable very short desorption lifetime predicted by DFT calculations[11,26] ($\tau_{d,O_3} = 3$ ns) in line with the potential energy diagram of Fig. 2, the observations can be matched only with a multistep LH reaction mechanism that involves the formation of ROIs with long lifetimes ($\sim 10^2$ s, see Supplementary Section S1). A simple LH mechanism with short O_3-desorption lifetimes and without the formation of long-lived ROIs would lead to a linear concentration dependence

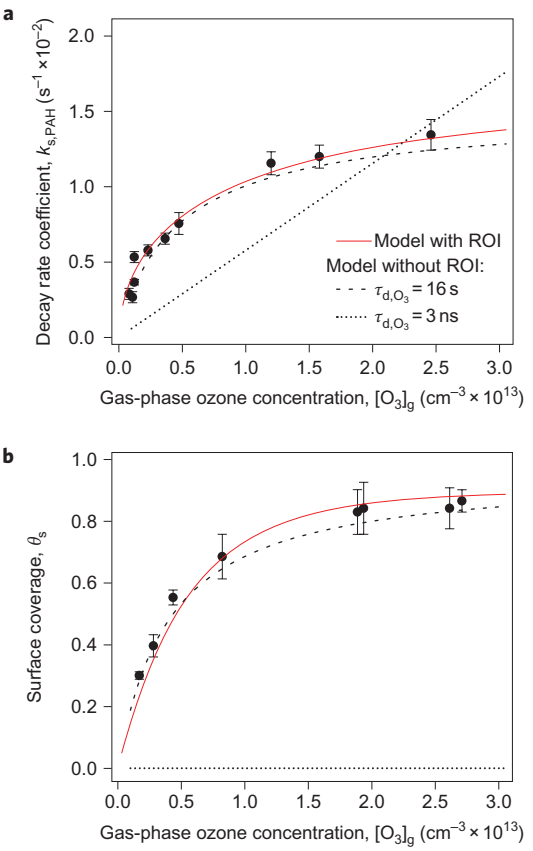

Figure 3 | Experimental and model results for heterogeneous ozonolysis of the PAH BaP on soot aerosol particles. a,b, Pseudo first-order decay rate coefficient for BaP ($k_{s,PAH}$) (**a**) and surface coverage (θ_s) (**b**) by physisorbed and chemisorbed O_3 as a function of gas-phase O_3 concentration ($[O_3]_g$). The data points and error bars represent experimental data and standard deviations[12]. The red line is from a model with ROI formation using a desorption lifetime for O_3 (τ_{d,O_3}) of 3 ns. The black lines are from models without ROI formation and with τ_{d,O_3} of 3 ns (dotted line) or 16 s (dashed line).

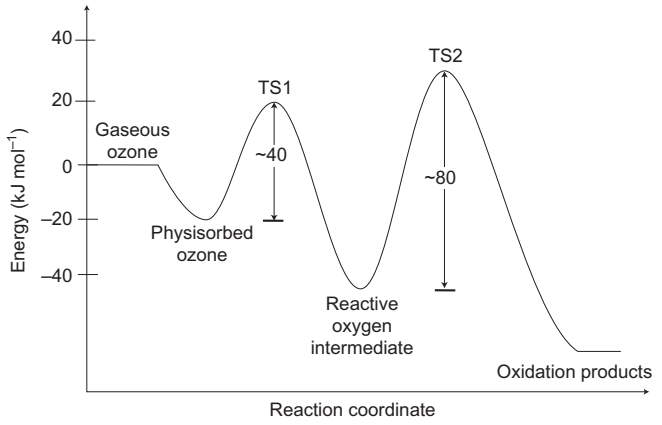

Figure 4 | Energy profile for the reaction of O_3 with the PAH BaP on soot. The ROI may be regarded as a chemisorbed oxygen atom. TS1 is the transition state from physisorbed O_3 to the ROI, which may be regarded as a trioxyl diradical or primary ozonide. TS2 is the transition state from the ROI to the oxidation products (oxygenated PAH), which may be regarded as an oxy or peroxy radical.

of $k_{s,PAH}$ on $[O_3]_g$ and to an unrealistically low surface coverage ($\theta_s = 10^{-6}$, Fig. 3b).

From the kinetic model approach using a multistep LH reaction mechanism, we derived an activation energy of $E_{a,pc} = \sim 41(\pm 7)$ kJ mol^{-1} for the transition from the physisorbed O_3 molecules to the ROI. This is consistent with the range of activation energies estimated from DFT calculations for the chemisorption of O_3 on PAHs and graphene (~40–100 kJ mol^{-1}) (refs 11,26). The activation energy from a ROI to oxidation products was estimated to be ~80(±9) kJ mol^{-1} (Supplementary Section S1.3, equation (20)). Accordingly, the energy profile of the heterogeneous reaction between O_3 and PAH that involves ROI formation can be described as shown in Fig. 4. The explicit inclusion of long-lived ROIs in a kinetic model allows us, for the first time, to reconcile the thermodynamic data of DFT calculations with the results of experimental studies to investigate the interaction of O_3 with aromatic surfaces.

ROIs in the nitration of protein. Also, strong evidence for the formation of long-lived ROIs from the interaction of O_3 with aerosol particles is provided by new experimental results on the nitration by NO_2 of the aromatic amino acid tyrosine in protein macromolecules. The uptake of NO_2 by protein particles was investigated in an aerosol flow tube using a short-lived radioactive tracer technique (^{13}N) (ref. 34) and bovine serum albumin (BSA), a globular protein with a molecular mass of 67 kDa and 21 tyrosine residues per molecule. The experimental methods are described below and in Supplementary Section S2.

As shown in Fig. 5, the NO_2 uptake coefficient (γ_{NO_2}) of BSA particles that were not in contact with O_3 was less than the detection limit (~10^{-6}), which is consistent with previous studies that indicate protein nitration by NO_2 alone is very slow[18]. However, when the BSA particles were pretreated with O_3 (97 parts per 10^9 (ppb)) and then exposed to NO_2 in the absence of O_3, a very efficient uptake of NO_2 was observed, with uptake coefficients that decreased with increases in NO_2 concentration from $\gamma_{NO_2} \approx 5 \times 10^{-4}$ at 6 ppb NO_2 to $\gamma_{NO_2} \approx 1 \times 10^{-4}$ at 27 ppb NO_2. The high reactivity of NO_2 with O_3-pretreated particles can be explained by a nitration reaction that involves O_3-generated ROIs – most likely phenoxy radical derivatives of tyrosine (Supplemetray Section S2.6)[35,36]. The decrease of γ_{NO_2} with increasing NO_2 concentration can be explained by the increasing consumption of ROIs. With concomitant exposure to O_3 (97 ppb), NO_2 uptake was still substantial, but γ_{NO_2} was lower, which can be attributed to competitive adsorption and reaction ($\gamma_{NO_2} \approx 5 \times 10^{-5}$). The rapid NO_2 uptake by pretreated BSA particles confirms that the reaction involves O_3-generated ROIs and is not dominated by alternative reaction pathways (reaction with NO_3 and N_2O_5 formed in the gas phase).

To examine the lifetime of the ROIs formed by O_3 on the proteins, we introduced a dead volume after the removal of O_3 and before the exposure of pretreated BSA particles to NO_2. We varied the time between O_3 pretreatment and NO_2 exposure over the range 250–550 s, but we observed no significant decrease of γ_{NO_2} (Fig. 6). This implies that the ROIs are long-lived and exhibit no significant decay on a timescale of ten minutes. The observed γ_{NO_2} results imply that proteins on the surface of aerosol particles are nitrated efficiently, within minutes, under photochemical smog conditions with high concentrations of O_3 and NO_2. The final products of the nitration reaction are nitrotyrosine residues in the protein macromolecule[18,37,38].

ROIs in other atmospheric surface and multiphase processes. Besides PAH oxidation and protein nitration, long-lived ROIs also appear to influence the reaction rates of O_3 with other surfaces, including olefinic and inorganic substrates (such as mineral dust), which exhibit similar LH reaction kinetics[9,10]. The ozonolysis of olefins may involve ozonides or stabilized Criegee intermediates[39,40], and the formation of atomic oxygen and peroxides was invoked to explain the kinetics of O_3 decomposition on mineral dust[41–43]. The chemical identity of O_3-generated ROIs probably varies with the nature of the substrate, but their formation energetics, given by the decomposition of adsorbed O_3 molecules, are probably similar for many substrates. They need to be long-lived to explain the LH reaction kinetics observed on interaction of O_3 with aerosol particles.

Apart from the chemical ageing of air particulate matter, long-lived ROIs may also participate in the formation and growth of secondary organic aerosols. In particular, surface interactions of long-lived ROIs may lead to the formation of multifunctional organic substances (acids, nitrates, sulfates, dimers, oligomers and so on) with the high molecular mass and low vapour pressure required for the nucleation and growth of new particles, and they may also influence their phase state[44–48]. Further investigations are required to unravel individual molecular species and steps involved

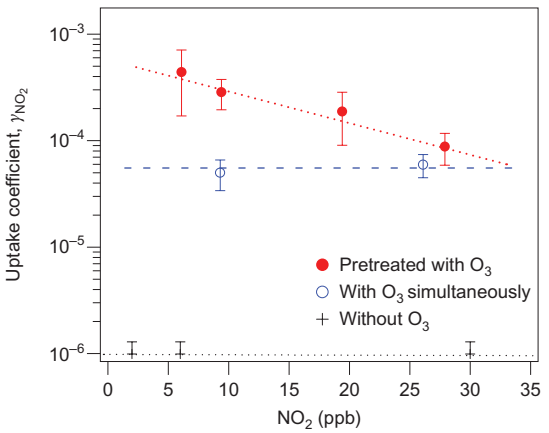

Figure 5 | Uptake coefficients of NO_2 by protein particles. These were exposed only to NO_2 (black crosses), exposed to 97 ppb O_3 and NO_2 at the same time (blue circles) or first pretreated with 97 ppb O_3 and then exposed to NO_2 (red circles). The data points and error bars represent experimental data and standard deviations. The lines are to guide the eye and illustrate that the NO_2 uptake is below the detection limit without O_3 (black), significant in the presence of O_3 (blue) and highest after pretreatment with O_3 (red).

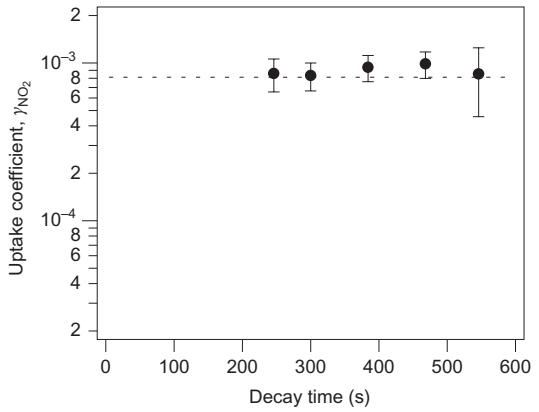

Figure 6 | Uptake coefficients of NO_2 by O_3-pretreated protein particles. These are plotted against the decay time after which the pretreated particles were exposed to NO_2. The data points and error bars represent experimental data and standard deviations. The line illustrates that the NO_2 uptake is quasi-constant up to about ten minutes, which confirms that the O_3-generated ROIs are long-lived.

in the processes outlined above, as well as their relative importance. The experimental and theoretical information currently available suggests that long-lived O_3-generated ROIs play a central role in the multiphase chemistry of atmospheric aerosols.

Methods

PAH oxidation. The kinetic double-layer model applied to model PAH oxidation (K2-SURF)[24] is based on the Pöschl–Rudich–Ammann framework for aerosol and cloud surface chemistry and gas–particle interactions[49,50]. It describes the gas–particle interface by using several compartments and molecular layers in which volatile and non-volatile species can undergo mass transport and chemical reactions: gas phase, near-surface gas phase, sorption layer and quasi-static surface layer. The chemical mechanisms and derivations of kinetic parameters are described in Supplementary Section S1. The surface mass balance and rate equations of surface species were solved numerically.

Protein nitration. Aerosols were generated by nebulizing an aqueous solution of BSA. The size distribution and surface area of particles were monitored by a scanning mobility particle sizer. Gas and particle flows were mixed in a cylindrical perfluoroalkoxy polymer flow tube. For the O_3 pretreatment experiments, O_3 was removed from the aerosol flow using potassium iodide denuder before mixing with NO_2. Afterwards, the flow entered a narrow parallel-plate diffusion denuder train coated to absorb the gas-phase NO_2 selectively, and then passed through a particle filter to collect the particles. The gamma-radiation detectors were attached to each denuder section and to the filters to detect the amount of emitted gamma quanta in the decay of ^{13}N, which corresponds to the amount of trapped ^{13}N molecules of a given species.

Received 19 October 2010; accepted 14 January 2011; published online 20 February 2011

References

1. Venkatachari, P. & Hopke, P. K. Development and evaluation of a particle-bound reactive oxygen species generator. *J. Aerosol. Sci.* **39,** 168–174 (2008).
2. Apel, K. & Hirt, H. Reactive oxygen species: metabolism, oxidative stress, and signal transduction. *Annu. Rev. Plant. Biol.* **55,** 373–399 (2004).
3. Finkel, T. & Holbrook, N. J. Oxidants, oxidative stress and the biology of ageing. *Nature* **408,** 239–247 (2000).
4. Mittler, R. Oxidative stress, antioxidants and stress tolerance. *Trends Plant Sci.* **7,** 405–410 (2002).
5. Pöschl, U. Atmospheric aerosols: composition, transformation, climate and health effects. *Angew. Chem. Int. Ed.* **44,** 7520–7540 (2005).
6. George, I. J. & Abbatt, J. P. D. Heterogeneous oxidation of atmospheric aerosol particles by gas-phase radicals. *Nature Chem.* **2,** 713–722 (2010).
7. Finlayson-Pitts, B. J. & Pitts, J. N. *Chemistry of the Upper and Lower Atmosphere* (Academic Press, 2000).
8. Seinfeld, J. H. & Pandis, S. N. *Atmospheric Chemistry and Physics – From Air Pollution to Climate Change* (John Wiley, 1998).
9. Finlayson-Pitts, B. J. Reactions at surfaces in the atmosphere: integration of experiments and theory as necessary (but not necessarily sufficient) for predicting the physical chemistry of aerosols. *Phys. Chem. Chem. Phys.* **11,** 7760–7779 (2009).
10. McCabe, J. & Abbatt, J. P. D. Heterogeneous loss of gas-phase ozone on *n*-hexane soot surfaces: similar kinetics to loss on other chemically unsaturated solid surfaces. *J. Phys. Chem. C* **113,** 2120–2127 (2009).
11. Maranzana, A. *et al.* Ozone interaction with polycyclic aromatic hydrocarbons and soot in atmospheric processes: theoretical density functional study by molecular and periodic methodologies. *J. Phys. Chem. A* **109,** 10929–10939 (2005).
12. Pöschl, U., Letzel, T, Schauer, C. & Niessner, R. Interaction of ozone and water vapor with spark discharge soot aerosol particles coated with benzo[*a*]pyrene: O_3 and H_2O adsorption, benzo[*a*]pyrene degradation, and atmospheric implications. *J. Phys. Chem. A* **105,** 4029–4041 (2001).
13. Kolb, C. E. *et al.* An overview of current issues in the uptake of atmospheric trace gases by aerosols and clouds. *Atmos. Chem. Phys.* **10,** 10561–10605 (2010).
14. Rudich, Y., Donahue, N. M. & Mentel, T. F. Aging of organic aerosol: bridging the gap between laboratory and field studies. *Annu. Rev. Phys. Chem.* **58,** 321–352 (2007).
15. Chu, S. N. *et al.* Ozone oxidation of surface-adsorbed polycyclic aromatic hydrocarbons: role of PAH–surface interaction. *J. Am. Chem. Soc.* **132,** 15968–15975 (2010).
16. Nel, A. Air pollution-related illness: effects of particles. *Science* **308,** 804–806 (2005).
17. Pöschl, U. Formation and decomposition of hazardous chemical components contained in atmospheric aerosol particles. *J. Aerosol. Med.* **15,** 203–212 (2002).
18. Franze, T., Weller, M. G., Niessner, R. & Pöschl, U. Protein nitration by polluted air. *Environ. Sci. Technol.* **39,** 1673–1678 (2005).
19. Fröhlich-Nowoisky, J., Pickersgill, D. A., Despres, V. R. & Pöschl U. High diversity of fungi in air particulate matter. *Proc. Natl Acad. Sci. USA* **106,** 12814–12819 (2009).
20. Yang, H., Zhang, Y. & Pöschl, U. Quantification of nitrotyrosine in nitrated proteins. *Anal. Bioanal. Chem.* **397,** 879–886 (2010).
21. Gruijthuijsen, Y. K. *et al.* Nitration enhances the allergenic potential of proteins. *Int. Arch. Allergy Immunol.* **141,** 265–275 (2006).
22. Traidl-Hoffmann, C., Jakob, T. & Behrendt, H. Determinants of allergenicity. *J. Allergy Clin. Immunol.* **123,** 558–566 (2009).
23. Ammann, M., Pöschl, U. & Rudich, Y. Effects of reversible adsorption and Langmuir–Hinshelwood surface reactions on gas uptake by atmospheric particles. *Phys. Chem. Chem. Phys.* **5,** 351–356 (2003).
24. Shiraiwa, M., Garland, R. M. & Pöschl, U. Kinetic double-layer model of aerosol surface chemistry and gas-particle interactions (K2-SURF): degradation of polycyclic aromatic hydrocarbons exposed to O_3, NO_2, H_2O, OH and NO_3. *Atmos. Chem. Phys.* **9,** 9571–9586 (2009).
25. Kwamena, N. O. A. *et al.* Role of the aerosol substrate in the heterogeneous ozonation reactions of surface-bound PAHs. *J. Phys. Chem. A* **111,** 11050–11058 (2007).
26. Lee, G., Lee, B., Kim, J. & Cho, K. Ozone adsorption on graphene: *ab initio* study and experimental validation. *J. Phys. Chem. C* **113,** 14225–14229 (2009).
27. Lennard-Jones, J. E. Processes of adsorption and diffusion on solid surfaces. *Trans. Faraday Soc.* **28,** 333–358 (1932).
28. Giordana, A. *et al.* Soot platelets and PAHs with an odd number of unsaturated carbon atoms and pi electrons: theoretical study of their spin properties and interaction with ozone. *J. Phys. Chem. A* **112,** 973–982 (2008).
29. Stephens, S., Rossi, M. J. & Golden D. M. The heterogeneous reaction of ozone on carbonaceous surfaces. *Int. J. Chem. Kinet.* **18,** 1133–1149 (1986).
30. Rogaski, C. A., Golden, D. M. & Williams, L. R. Reactive uptake and hydration experiments on amorphous carbon treated with NO_2, SO_2, O_3, HNO_3, and H_2SO_4. *Geophys. Res. Lett.*, **24,** 381–384 (1997).
31. Sorescu, D. C., Jordan, K. D. & Avouris, P. Theoretical study of oxygen adsorption on graphite and the (8,0) single-walled carbon nanotube. *J. Phys. Chem. B* **105,** 11227–11232 (2001).
32. Kutana, A. & Giapis, K. P. First-principles study of chemisorption of oxygen and aziridine on graphitic nanostructures. *J. Phys. Chem. C* **113,** 14721–14726 (2009).
33. Paulot, F. *et al.* Unexpected epoxide formation in the gas-phase photooxidation of isoprene. *Science* **325,** 730–733 (2009).
34. Ammann, M. Using ^{13}N as tracer in heterogeneous atmospheric chemistry experiments. *Radiochim. Acta* **89,** 831–838 (2001).
35. Truong, H., Lomnicki, S. & Dellinger, B. Potential for misidentification of environmentally persistent free radicals as molecular pollutants in particulate matter. *Environ. Sci. Technol.*, **44,** 1933–1939 (2010).
36. Harrison, M. A. J. *et al.* Nitrated phenols in the atmosphere: a review. *Atmos. Environ.*, **39,** 231–248 (2005).
37. Zhang, Y., Yang, H. & Pöschl, U. Analysis of nitrated proteins and tryptic peptides by HPLC-chip-MS/MS: site-specific quantification, nitration degree, and reactivity of tyrosine residues. *Anal. Bioanal. Chem.* **399,** 459–477 (2011).
38. Walcher, W. *et al.* Liquid- and gas-phase nitration of bovine serum albumin studied by LC-MS and LC-MS/MS using monolithic columns. *J. Proteome Res.* **2,** 534–542 (2003).

39. Baker, J., Aschmann, S. M., Arey, J. & Atkinson, R. Reactions of stabilized Criegee intermediates from the gas-phase reactions of O_3 with selected alkenes. *Int. J. Chem. Kinet.* **34,** 73–85 (2001).
40. Dubowski, Y. *et al.* Interaction of gas-phase ozone at 296 K with unsaturated self-assembled monolayers: a new look at an old system. *J. Phys. Chem. A* **108,** 10473–10485 (2004).
41. Li, W., Gibbs, G. V. & Oyama, S. T. Mechanism of ozone decomposition on a manganese oxide catalyst. I. *In situ* Raman spectroscopy and *ab initio* molecular orbital calculations. *J. Am. Chem. Soc.* **120,** 9041–9046 (1998).
42. Sullivan, R. C., Thornberry, T. & Abbatt, J. P. D. Ozone decomposition kinetics on alumina: effects of ozone partial pressure, relative humidity and repeated oxidation cycles. *Atmos. Chem. Phys.* **4,** 1301–1310 (2004).
43. Hanisch, F. & Crowley, J. N. Ozone decomposition on Saharan dust: an experimental investigation. *Atmos. Chem. Phys.* **3,** 119–130 (2003).
44. Hallquist, M. *et al.* The formation, properties and impact of secondary organic aerosol: current and emerging issues. *Atmos. Chem. Phys.* **9,** 5155–5235 (2009).
45. Jimenez, J. L. *et al.* Evolution of organic aerosols in the atmosphere. *Science* **326,** 1525–1529 (2009).
46. Virtanen, A. *et al.* An amorphous solid state of biogenic secondary organic aerosol particles. *Nature* **467,** 824–827 (2010).
47. Pöschl, U. *et al.* Rainforest aerosols as biogenic nuclei of clouds and precipitation in the Amazon. *Science* **329,** 1513–1516 (2010).
48. Kalberer, M. *et al.* Identification of polymers as major components of atmospheric organic aerosols. *Science* **303,** 1659–1662 (2004).
49. Pöschl, U., Rudich, Y. & Ammann, M. Kinetic model framework for aerosol and cloud surface chemistry and gas–particle interactions. Part 1: General equations, parameters, and terminology. *Atmos. Chem. Phys.* **7,** 5989–6023 (2007).
50. Ammann, M. & Pöschl, U. Kinetic model framework for aerosol and cloud surface chemistry and gas–particle interactions. Part 2: Exemplary practical applications and numerical simulations. *Atmos. Chem. Phys.* **7,** 6025–6045 (2007).

Acknowledgements

This work was funded by the Max Planck Society, the Swiss National Science Foundation (Grant 130175) and the European Integrated Project on Aerosol, Cloud, Climate and Air Quality Interactions (036833-2 EUCAARI). We thank M. Birrer, T. Bartels-Rausch and M. Kerbrat for support, and the staff of the Paul Scherrer Institute accelerator facilities for providing the stable proton beams used to produce ^{13}N with the PROTRAC facility. M.S. is supported by the Max Planck Graduate Center, Johannes Gutenberg University Mainz, the University of Tokyo, and the Ministry of Education, Culture, Sports, Science and Technology, Japan.

Author contributions

U.P., M.A. and M.S. designed the research. M.S., Y.S., A.R. and M.A. performed tracer experiments and M.S. analysed the data. H.Y. and Y.Z. contributed to the protein studies. M.S. and U.P. conducted the kinetic modelling. M.S., U.P., M.A. and J.A. discussed the results. M.S., U.P. and M.A. co-wrote the paper.

Additional information

The authors declare no competing financial interests. Supplementary information accompanies this paper at www.nature.com/naturechemistry. Reprints and permission information is available online at http://npg.nature.com/reprintsandpermissions/. Correspondence and requests for materials should be addressed to U.P.